

N O T I C E

THIS DOCUMENT HAS BEEN REPRODUCED FROM
MICROFICHE. ALTHOUGH IT IS RECOGNIZED THAT
CERTAIN PORTIONS ARE ILLEGIBLE, IT IS BEING RELEASED
IN THE INTEREST OF MAKING AVAILABLE AS MUCH
INFORMATION AS POSSIBLE



Annual Status Report

NASA Grant NSG 7386

LABORATORY STUDIES OF ATOMIC COLLISION PROCESSES
OF IMPORTANCE IN PLANETARY ATMOSPHERES

R.F. Stebbings and Ken Smith
Rice University

Period ending 31 August, 1985

NR6-12019

ENCLOS
27649

63/12

(NASA-CR-170301) LABORATORY STUDIES OF
ATOMIC COLLISION PROCESSES OF IMPORTANCE IN
PLANETARY ATMOSPHERES Annual Status Report
(NASA-111V.) 25 P HC A02/MF A01 CSCL 20H

During the year ending on 31 August, 1985, the research supported under NSG 7386 has included:

- I. Measurement of differential cross sections for atomic collision processes relevant to analysis and modeling of data from NASA Missions Pioneer 11, Pioneer 12, Voyager 1, and Voyager 2. Specifically, this work includes:
 - A) differential charge-transfer cross sections for ground-state O^+ projectiles colliding with N_2 , O_2 , CO_2 , SO_2 , H_2 , and He,
 - B) differential charge-transfer cross sections for excited-state $O^+(^2D)$ ions colliding with N_2 and O_2 , and
 - C) differential cross sections for angular scattering of O atoms by H_2 , N_2 , O_2 , and He targets.
- II. Development and initial use of apparatus to study large-angle scattering using coincidence techniques.
- III. Development of an apparatus to provide dense O-atom and H-atom targets for collision studies.

I. Differential cross sections

Using the apparatus shown in Figure 1, we have measured a variety of differential cross sections for angular scattering and charge transfer. These studies employ position-sensitive detectors (PSD's) to collect collision products scattered over a wide range of angles, and the research program includes investigation of differential cross sections for total angular scattering, charge transfer, stripping, and other collisions. All of these processes can be studied with the same basic apparatus, but minor modifications in the equipment details and in the data acquisition programs and techniques are required for each individual experiment.

A. Charge transfer of ground-state O^+ ions

The NASA missions to Jupiter have shown that the region of Io's orbit contains both a plasma torus of oxygen and sulfur ions, and substantial concentrations of atomic oxygen, atomic sulfur, and alkali metals. Recent modeling studies indicate that charge transfer and other atomic collision processes act to couple Jupiter's magnetosphere to the neutral gas cloud near Io's orbit. Several Jovian moons have substantial atmospheres, all of which interact by charge transfer with the energetic ions in Jupiter's magnetosphere. In addition, data from Voyager show that Saturn has a co-rotating magnetosphere, providing fast ions that are expected to interact with the atmospheres of Titan and Dione-Tethys. In all of these environments, charge-transfer collisions are the primary process through which energetic ions interact with neutral species, and many of the relevant cross sections for charge-transfer have not been measured.

During the last year, we have performed a series of charge-transfer measurements involving energetic O^+ ions:



Even though charge-transfer processes have been studied for many years, a search of the literature has revealed very few measurements of total cross sections for charge exchange of O^+ ions with other gases, and the results do not agree with one another. There have been no differential cross sections published for this process.

In regions of planetary atmospheres where the atom density is low and the mean time between collisions is long, most of the O^+ ions undergoing charge transfer will be in the ground (4S) state. In the present work we pay particular attention to production of a ground-state projectile beam. The ion source used produces a mixed beam of ground-state $O^+(^4S)$ and excited-state $O^+(^2D)$ ions. An additional gas cell (designated "filter cell" in Fig. 1) has been installed in the projectile beam path. This cell is filled with N_2 , which has a large charge-transfer cross section for excited projectile ions, but has a small charge-transfer cross section for ground-state species. When the beam passes through the cell, the excited-state ions are preferentially converted to fast neutral atoms, greatly increasing the ground-state fraction of the remaining ion beam. The performance of this "filtration" system has been optimized during the last year, and we now routinely produce beams having an excited-state fraction of less than 2%.

Experiments using the apparatus shown in Fig. 1 are particularly straightforward because the primary ion beam and the fast neutral atoms produced by charge-transfer collisions are both detected by the same position-sensitive detector (PSD). The PSD output is recorded under three circumstances.

- (1) no gas in target cell -- primary O^+ beam striking detector
- (2) gas in target cell -- mixed O^+ beam and O-atom product detected
- (3) gas in cell, deflection plates on -- O-atom product alone detected

If the relative efficiencies for detection of the O^+ projectiles and the O-atom products are known, the measurements (1) and (3) give the information necessary for ascertaining the differential scattering cross section. While the detection efficiencies for ions and atoms are similar, they are not necessarily the same at all projectile energies, and they must be measured. The detection efficiency measurement is also facilitated by the large solid angle subtended by the detector because almost all scattered ions and fast neutral atoms (produced by charge transfer) strike the detector surface. If all the fast scattered particles were collected, the relative detection efficiencies for ions and atoms could be determined trivially by:

- (i) measuring the count rate due to a known ion flux with no gas in the target cell;
- (ii) adding gas to the target cell in a sufficient amount to convert the ion flux to a fast neutral flux by charge transfer; and
- (iii) measuring the resulting neutral count rate.

The detection efficiency ratio for ions and atoms would simply be the ratio of the count rates measured with and without gas in the target cell. In practice, however, some of the fast ions and atoms are scattered enough to miss the detector, and it is not readily possible to completely convert an

ion flux to a neutral flux by charge transfer. To account for particles that miss the detector and for the partial conversion of the primary ion flux to fast neutrals, measurements (2) and (3) are taken at several different values of target cell pressure. The relative detection efficiencies for ions and atoms are ascertained from analysis of this data.

Measurements of differential charge-transfer cross sections for O^+ ions with N_2 , O_2 , CO_2 , SO_2 , H_2 , and He in the collision-energy range 500-5000 eV are now underway. Figures 2-7 give representative data for differential charge-transfer cross sections for ground-state O^+ ions colliding with these species at a lab-frame collision energy of 1500 eV.

B. Collision cross sections for excited ions.

The technique used for "filtering" the excited $O^+(^2D)$ out of the primary beam provides a simple means of measuring the charge-transfer cross sections for this species as well. We first make a measurement of the differential charge-transfer cross section for a beam containing a mixture of $O^+(^4S)$ and $O^+(^2D)$. By observing the ion current passing through the filter cell as a function of filter cell pressure, we can find the relative amounts of $O^+(^4S)$ and $O^+(^2D)$ present in the incident beam. With the filter cell operating at a pressure that permits passage of a predominantly ground-state beam, the differential cross section for charge transfer in the target cell is re-measured. Comparison of the results obtained for a mixed-state beam of known composition and those for the pure-ground-state beam yields the differential charge-transfer cross section for the excited $O^+(^2D)$ state. Figures 8 and 9 show comparisons of the measured differential cross sections for charge transfer of $O^+(^4S)$ and $O^+(^2D)$ with N_2 and O_2 , respectively. These data represent the first differential charge-transfer cross sections measured for an excited-state ion. The significant differences between the ground- and excited-state

differential cross sections for the N_2 target are consistent with the fact that the excited-state reaction is nearly energy-resonant, whereas the ground-state reaction is not.

C. Differential cross sections for angular scattering

When fast atomic particles (both ions and the fast neutrals produced by charge transfer) interact with planetary atmospheres, angular scattering is a primary means by which they transfer their kinetic energy to those atmospheres. Using the apparatus shown in fig 1, we have measured total differential cross sections for angular scattering (without regard to the products' electronic or charge states) of ground-state O-atoms by H_2 , N_2 , O_2 , and He in the collision energy range between 500 and 5000 eV. These data appear in Figures 10-13.

II. Apparatus development for large-angle scattering measurements

Analysis of the angular scattering data at small angles has shown that an unexpectedly-large fraction of the transfer of the fast particles' energy to the target particles occurs via large-angle scattering. We have therefore constructed the apparatus shown schematically in Figure 14 for measurement of large-angle scattering cross sections. In large-angle scattering, a significant amount of energy is transferred to the target particle, and both the initial projectile and the target leave the scattering region with significant energy. In the large-angle measurement we detect *both* particles arising from a single scattering event by using two position-sensitive detectors. Analysis of the data from these experiments can give both the differential cross section for large-angle scattering and the amount of energy going into internal excitation of the products.

Preliminary data for He-He collisions at large angles is shown in Figures 15 and 16. The structure in the data is due to known effects arising from the indistinguishability of the Helium nuclei in the collision process. When the nuclei are distinguishable (as in the case of $^3\text{He} - ^4\text{He}$ collisions shown in Fig. 16), oscillations in the cross section are not observed.

III. Atomic gas target

Atomic oxygen and atomic sulfur are significant constituents of Jupiter's extended atmosphere. Recent analyses of Voyager data suggest that there may be substantial densities of atomic hydrogen near Saturn. While atomic species are extremely important in many atmospheric applications, there have been relatively few experiments with them because they are so difficult to handle in the laboratory. During the last few months, we have assembled an apparatus for collision studies with a dense ($10^{15}/\text{cm}^3$) oxygen atom target. In this apparatus, molecular oxygen is dissociated by a microwave discharge, and flows through a coated quartz tube to the collision cell. We have performed several experiments to determine how effectively the atomic oxygen produced in the discharge is removed via collisions with various cell wall materials. The conclusion of this research is that one can readily achieve a gas mixture in the target cell that is about 50% atomic oxygen and about 50% molecular oxygen. At present, we determine the oxygen atom content of the reactant gas using a titration technique, observing light from a chemiluminescent reaction to monitor the titration. A time-of-flight mass spectrometer to monitor the relative concentrations of O and O_2 in the reaction cell is now under construction. The mass spectrometer will help to determine the effectiveness of the source in producing atomic species other than oxygen (*e.g.* sulfur and hydrogen). The oxygen target cell has been installed in the apparatus, and first experiments on charge transfer between O^+ ions and O-atoms will be performed within the next few weeks.

PUBLICATIONS :

Differential scattering cross sections for collisions of 0.5-, 1.5-, and 5.0 keV

Helium atoms with He, H₂, N₂, and O₂. J.H. Newman, K.A. Smith, R.F.

Stebbing, and Y. Chen. Accepted for publication, *J. Geophys. Res.* 1985.

Differential cross sections for scattering of 0.5-, 1.5-, and 5.0 keV

Hydrogen atoms with He, H₂, N₂, and O₂. J.H. Newman, Y. Chen, K.A. Smith,

R.F. Stebbing. To be submitted for publication, *J. Geophys. Res.* 1985.

Differential cross sections for scattering of 0.5-, 1.5-, and 5.0 keV Oxygen

atoms with He, H₂, N₂, and O₂. D.A. Schafer, J.H. Newman, K.A. Smith, R.F.

Stebbing. To be submitted for publication, *J. Geophys. Res.* 1985.

Laser-induced photodissociation of O₂⁺ and O₂, R.S. Gao, M.A. Thesis, Rice

University (1984)

Differential cross sections for neutral-neutral and charge-transfer

collisions, D.A. Schafer, Rice University (1985)

PRESENTATIONS:

Differential cross sections for charge transfer of O⁺ with atmospheric gases,

D.A. Schafer, J.H. Newman, K.A. Smith, and R.F. Stebbing, APS Division of

Electron and Atomic Physics Conference, Norman, OK (May, 1985).

Photofragment spectroscopy of $O_2(A)$ and $O_2(\Delta)$, R.S. Gao, Y.S. Chen, J.H. Newman, K.A. Smith, and R.F. Stebbings, APS Division of Electron and Atomic Physics Conference, Norman, OK (May, 1985).

Interaction potentials derived from neutral-neutral differential cross sections, J.H. Newman, K.A. Smith, and R.F. Stebbings, APS Division of Electron and Atomic Physics Conference, Norman, OK (May, 1985).

KeV-energy differential scattering: cross sections, interaction potentials and diffraction, J.H. Newman, D.A. Schafer, K.A. Smith, and R.F. Stebbings, International Conference on the Physics of Electron and Atomic Collisions, San Francisco, CA (July, 1985).

Differential charge-transfer cross sections for $O^+(^4S)$ and $O^+(^2D)$ ions with atmospheric gases, D.A. Schafer, J.H. Newman, K.A. Smith, and R.F. Stebbings, International Conference on the Physics of Electron and Atomic Collisions, San Francisco, CA (July, 1985).

Absolute cross sections for angular scattering of kilovolt-energy O and H atoms in collisions with atmospheric gases, R.F. Stebbings, K.A. Smith, J.H. Newman, and D.A. Schafer, American Geophysical Union Conference (December, 1985)

Angular scattering in atomic collisions, J.H. Newman, Physics colloquium University of Texas at Austin (November 1985)

Cross sections for charge transfer of O^+ ions with N_2 , K.A. Smith, R.F. Stebbings, J.H. Newman, and D.A. Schafer, American Geophysical Union Conference (December, 1985)

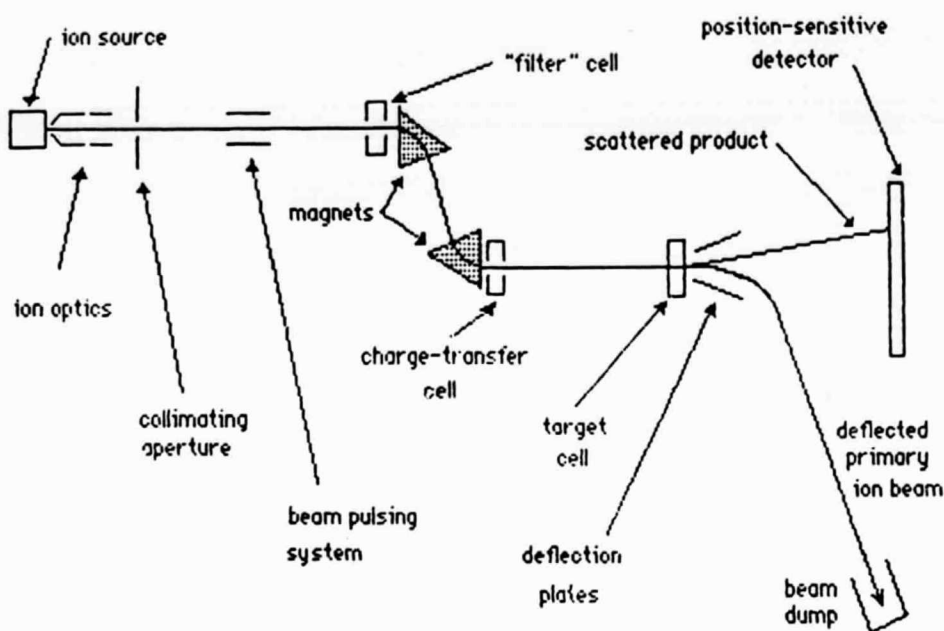


Fig. 1. Apparatus for differential cross section measurement. This machine will accommodate experiments with neutral or charged species. Selective removal of a state present in the incident beam is accomplished by filling the filter cell with gas having a large charge-transfer cross section for the state to be removed. If a fast neutral reactant beam is desired, the charge-transfer cell (CTC) is used; for studies of ion collisions, the CTC is empty.

O^+ (1500eV, S) + N_2

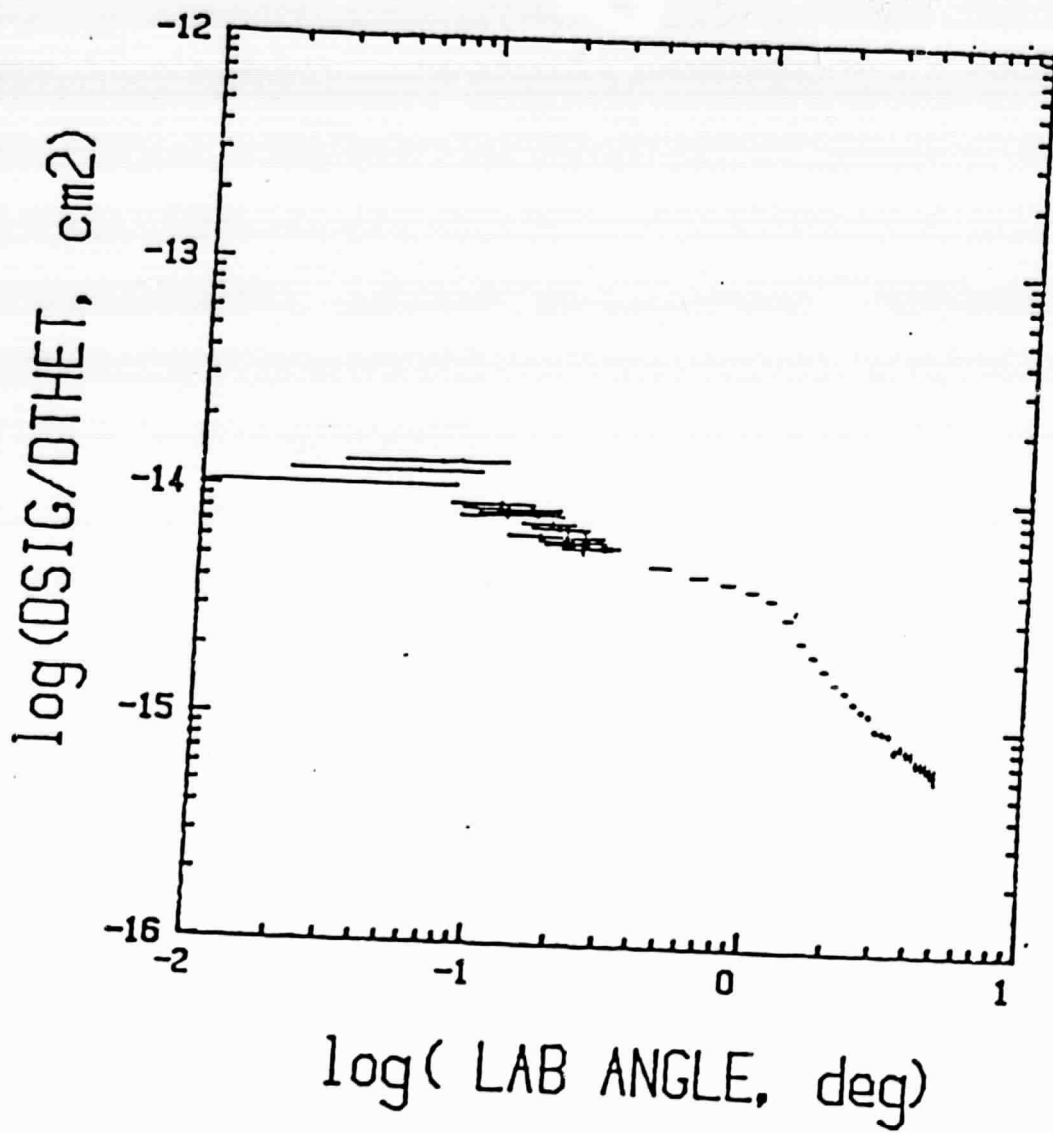


Fig. 2. Differential cross section for charge transfer between ground-state 1.5-keV O^+ ions and N_2 .

$O^+ (1500\text{eV}, {}^4S) + O_2$

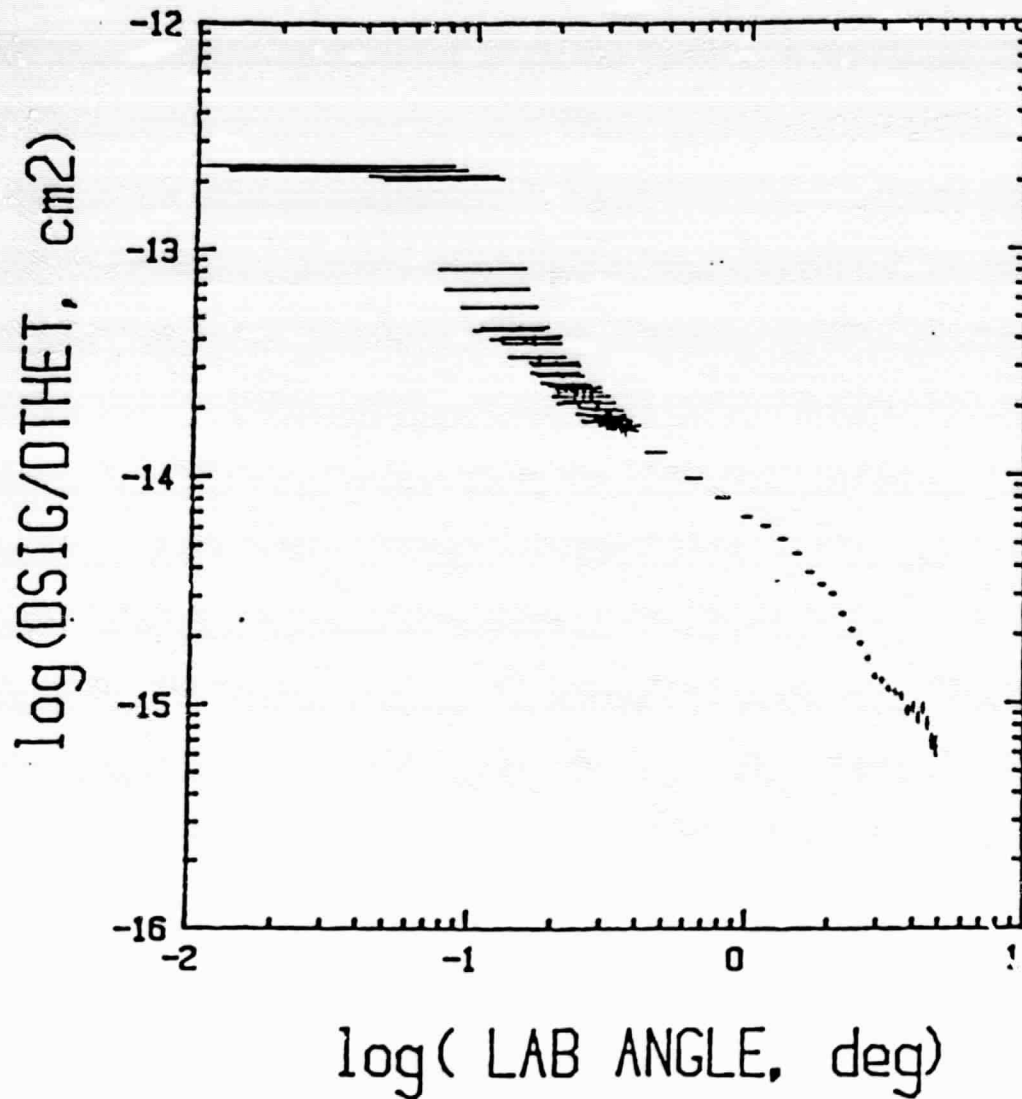


Fig. 3. Differential cross section for charge transfer between ground-state 1.5-keV O^+ ions and O_2 .

O^+ (1500eV, 4S) + CO_2

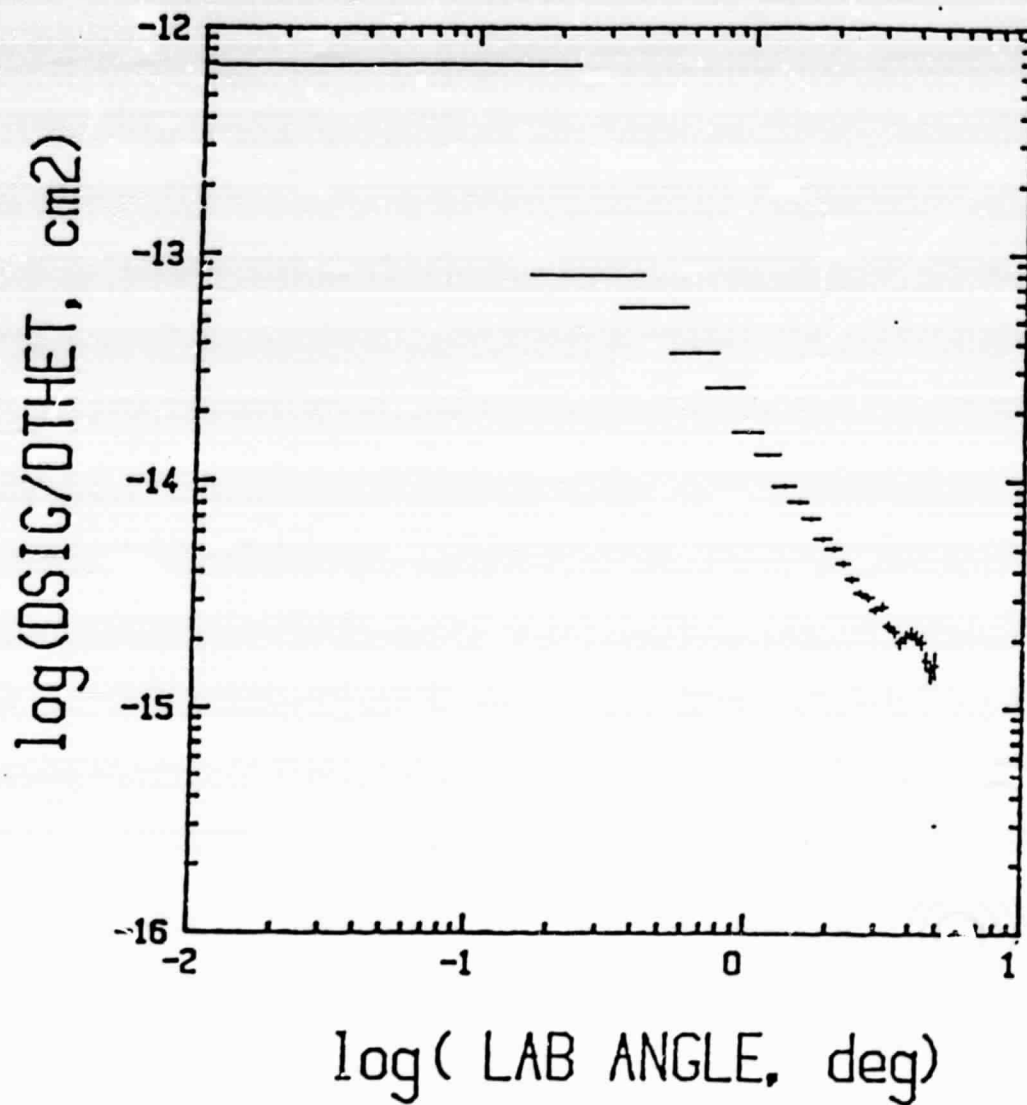


Fig. 4. Differential cross section for charge transfer between ground-state 1.5-keV O^+ ions and CO_2 .

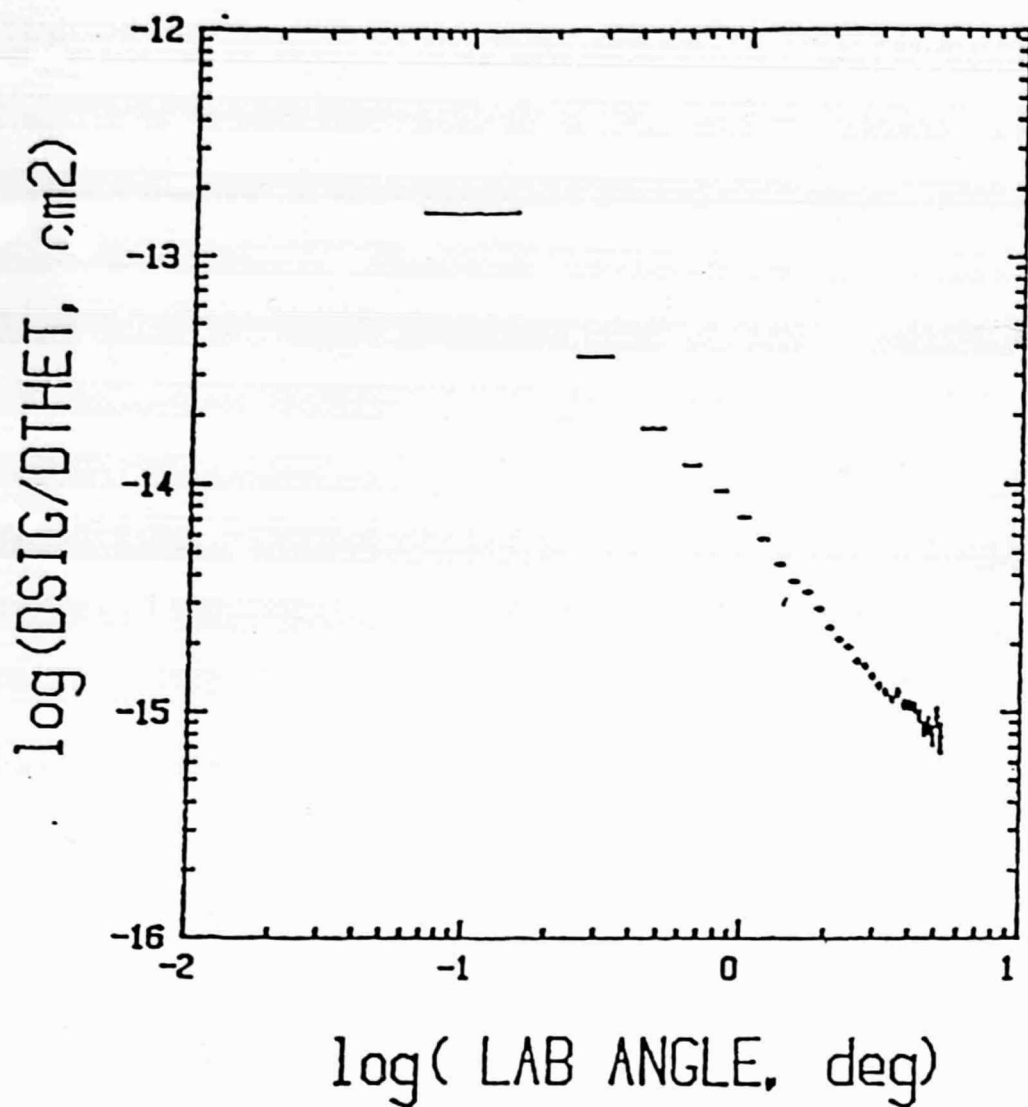
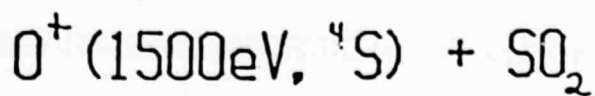


Fig. 5. Differential cross section for charge transfer between ground-state 15-keV O^+ ions and SO_2 .

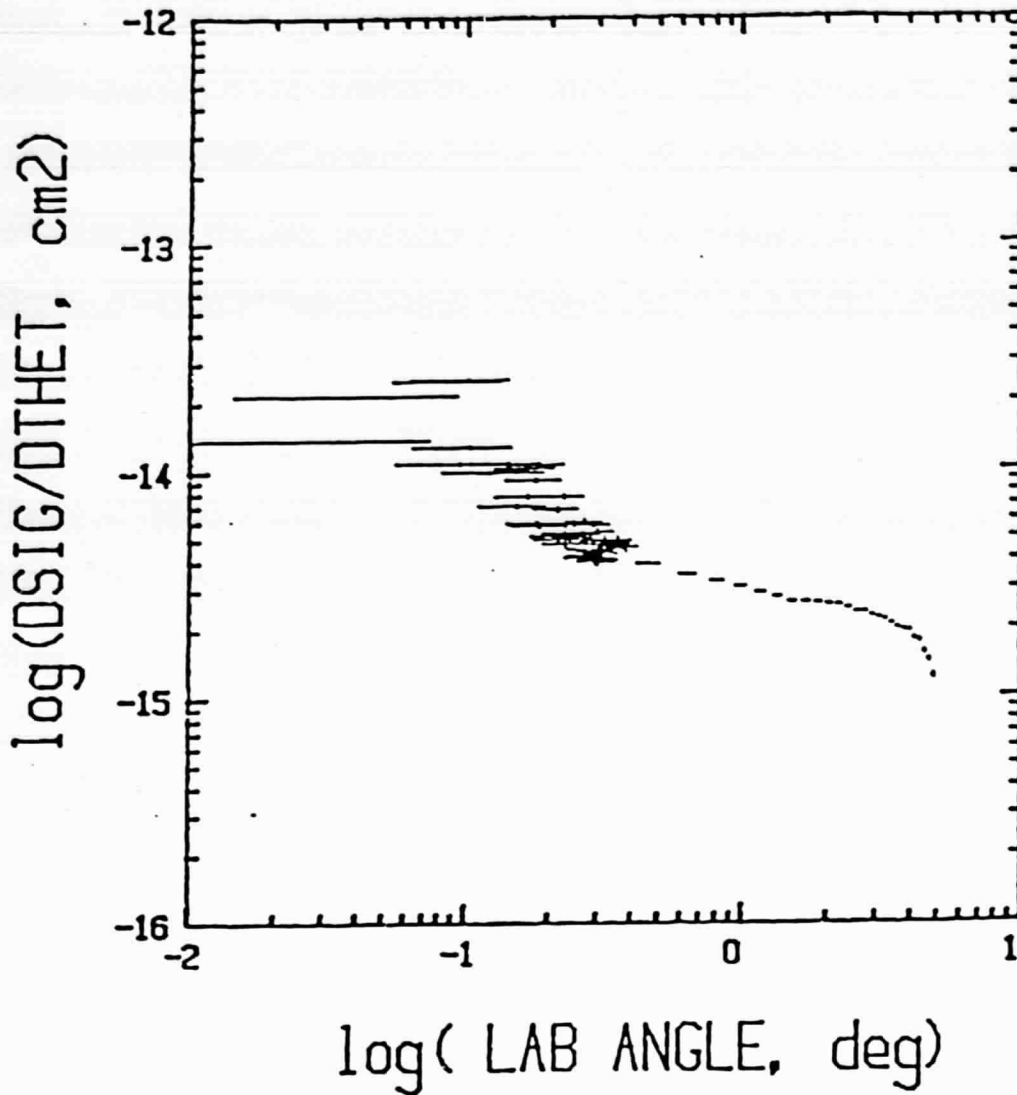
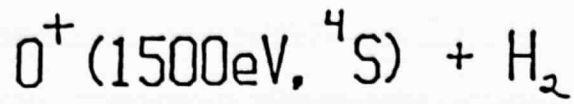


Fig. 6. Differential cross section for charge transfer between ground-state 1.5-keV O^+ ions and H_2 .

O^+ (1500eV, 4S) + He

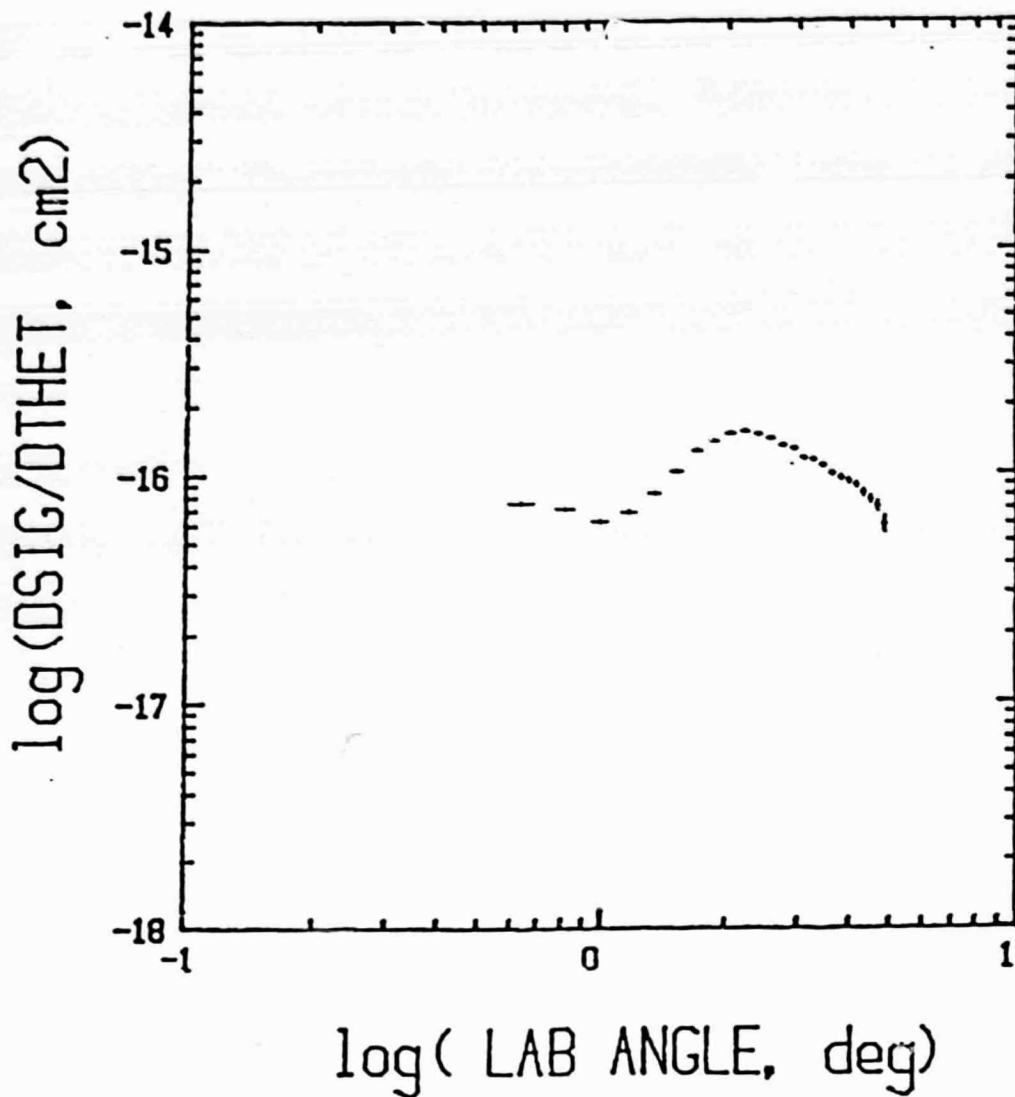


Fig. 7. Differential cross section for charge transfer between ground-state 1.5-keV O^+ ions and He.

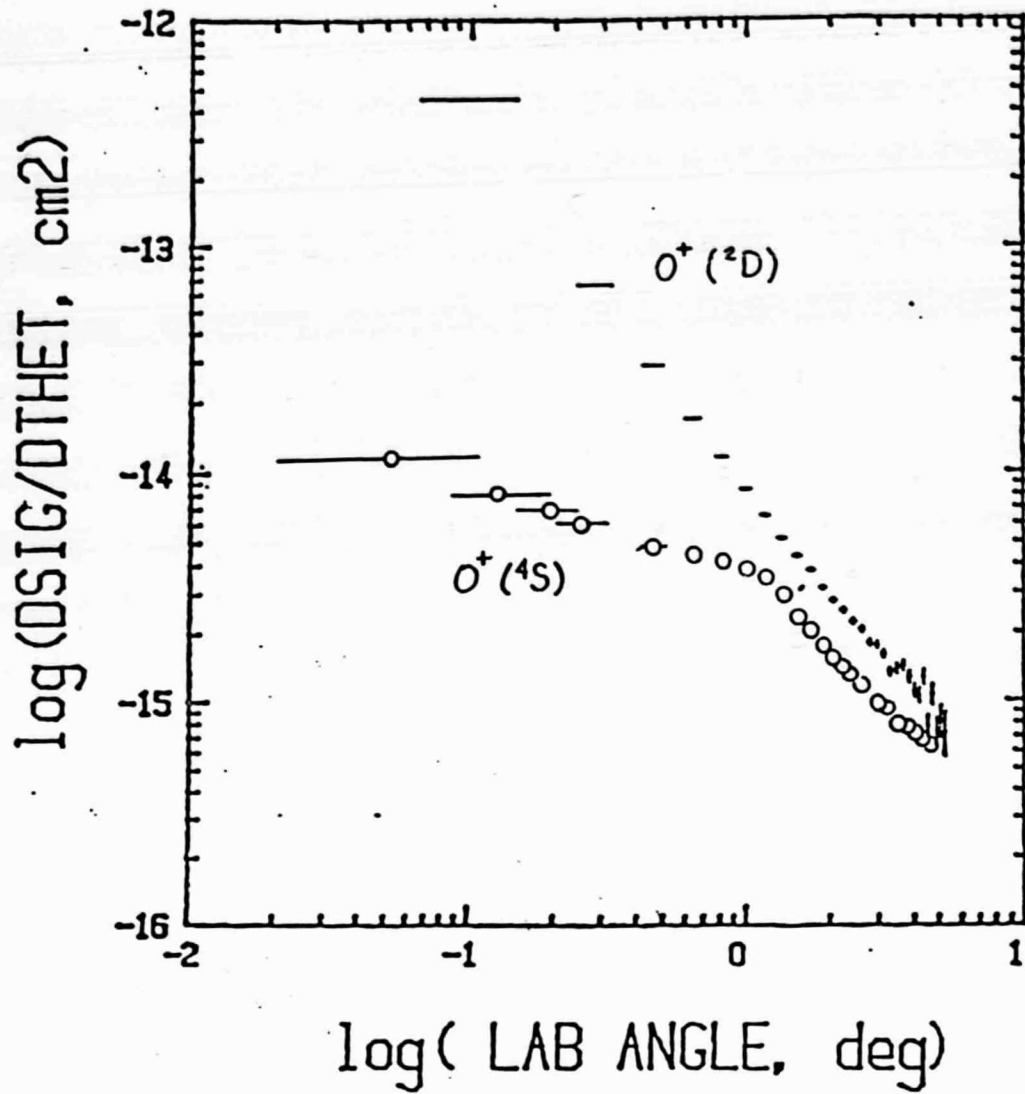


Fig. 8. Comparison of differential cross sections for charge transfer between ground-state and excited-state 1.5-keV O^+ ions and N_2 .

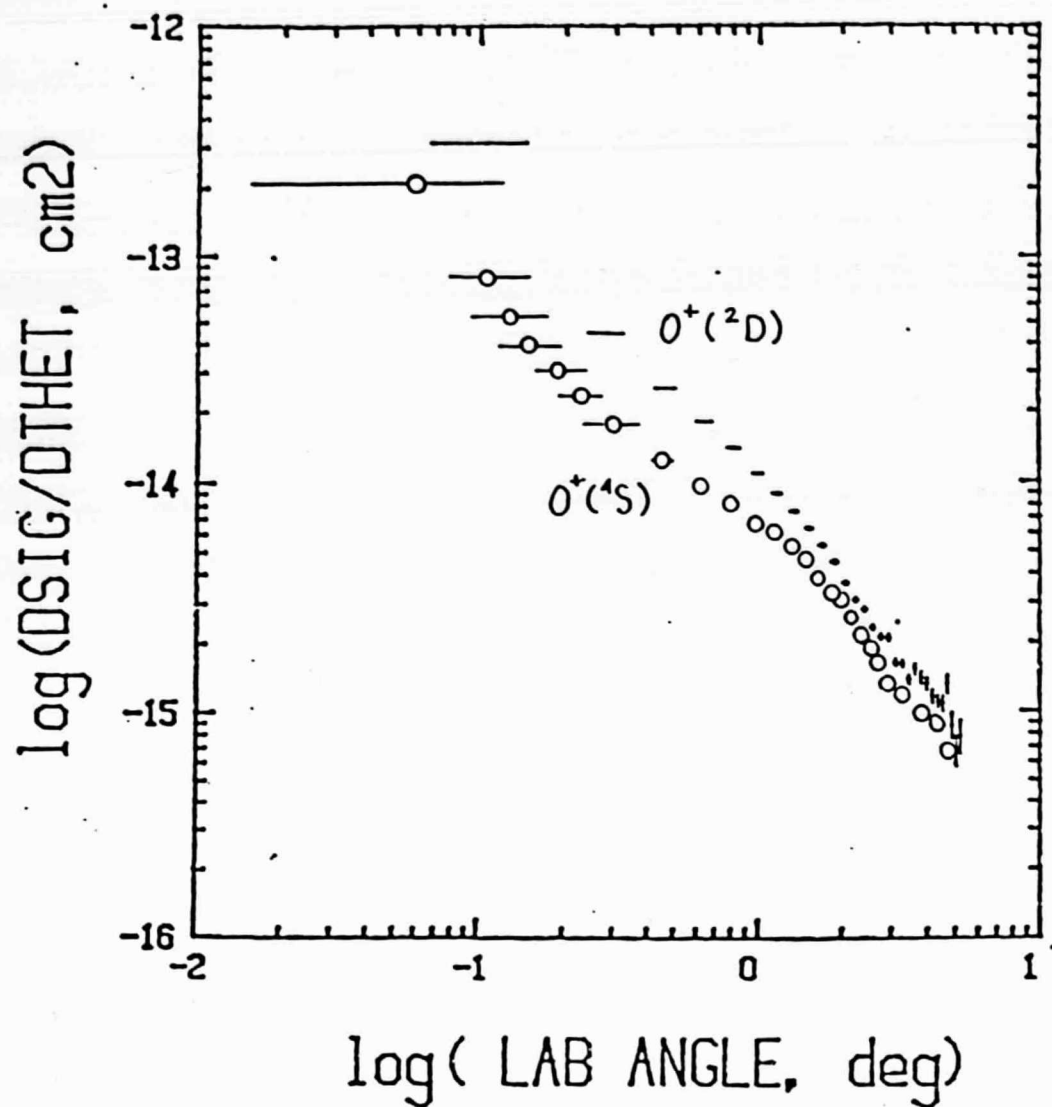


Fig. 9. Comparison of differential cross sections for charge transfer between ground-state and excited-state 1.5-keV O^+ ions and O_2 .

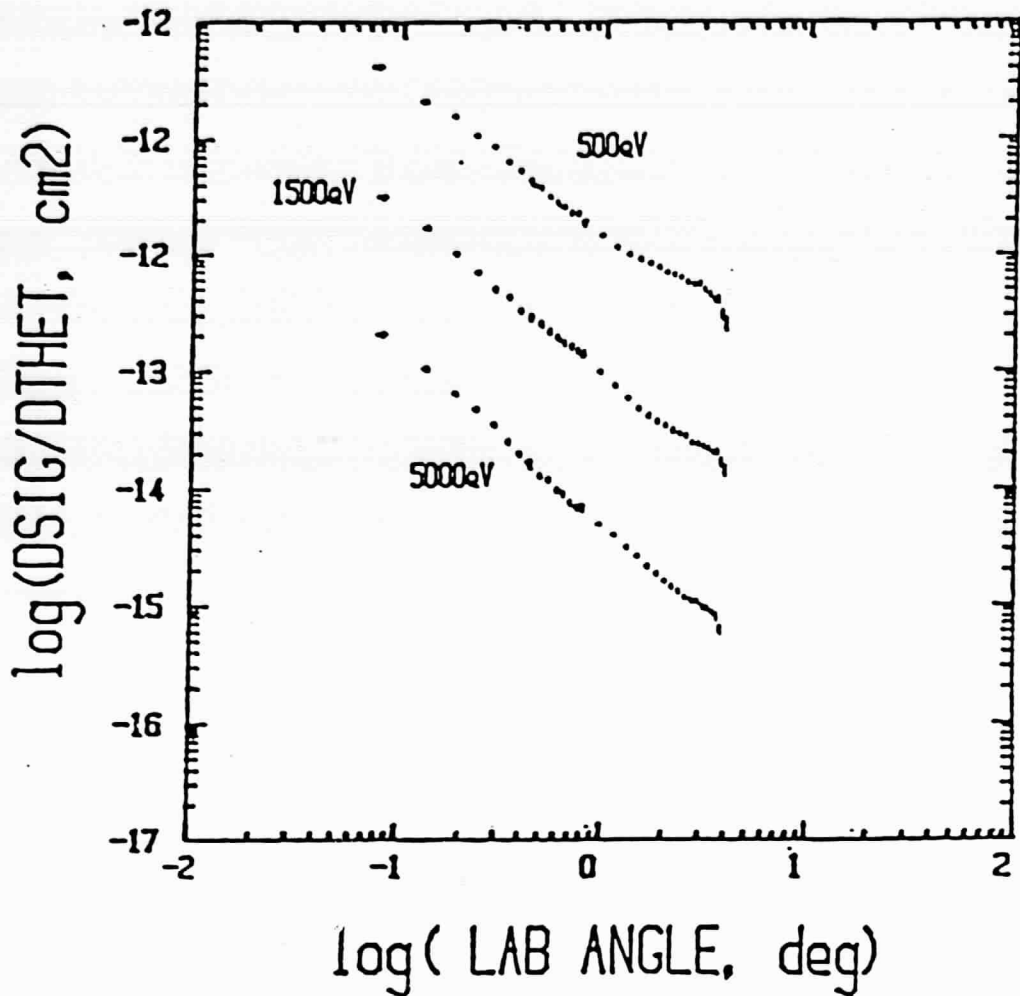
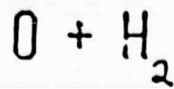


Fig. 10. Differential cross sections for angular scattering of ground-state 0.5-, 1.5-, and 5-keV oxygen atoms by H₂.

O + N₂

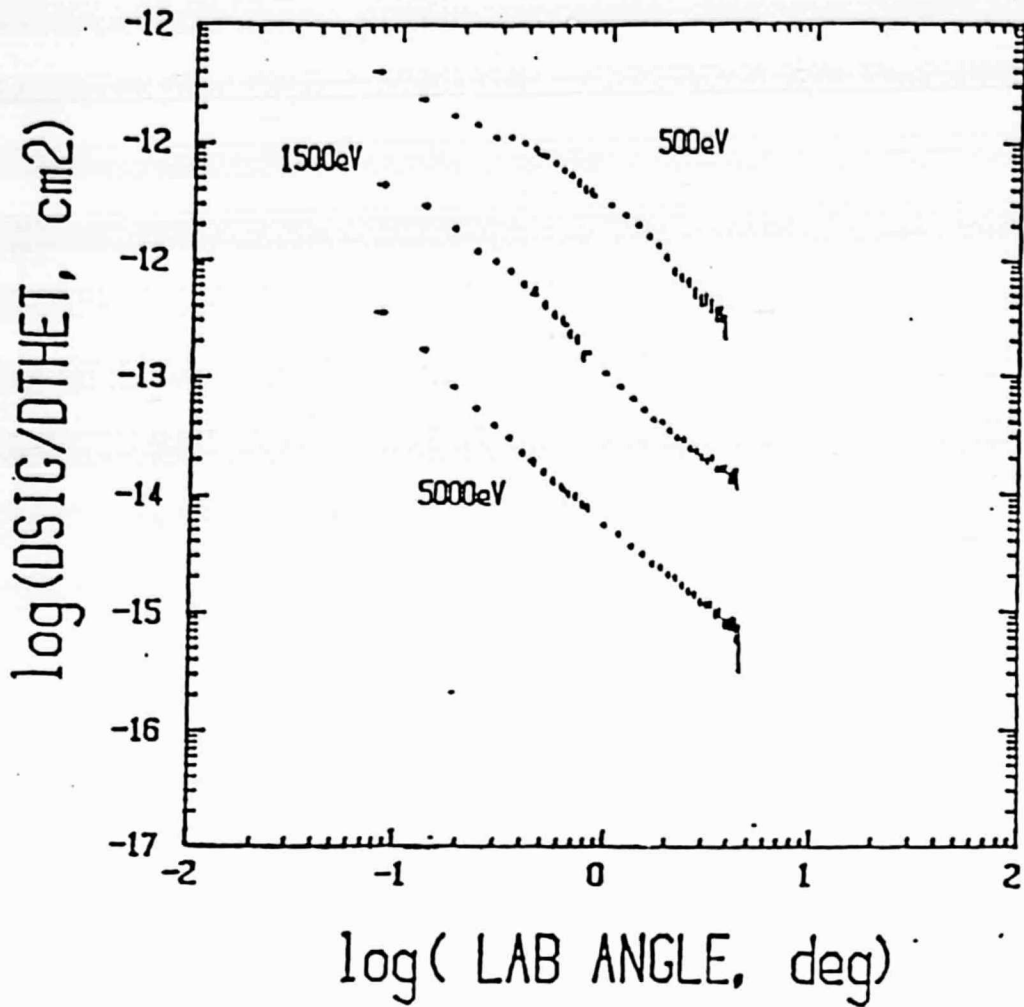


Fig. 11. Differential cross sections for angular scattering of ground-state 0.5-, 1.5-, and 5-keV oxygen atoms by N₂.

0 + 02

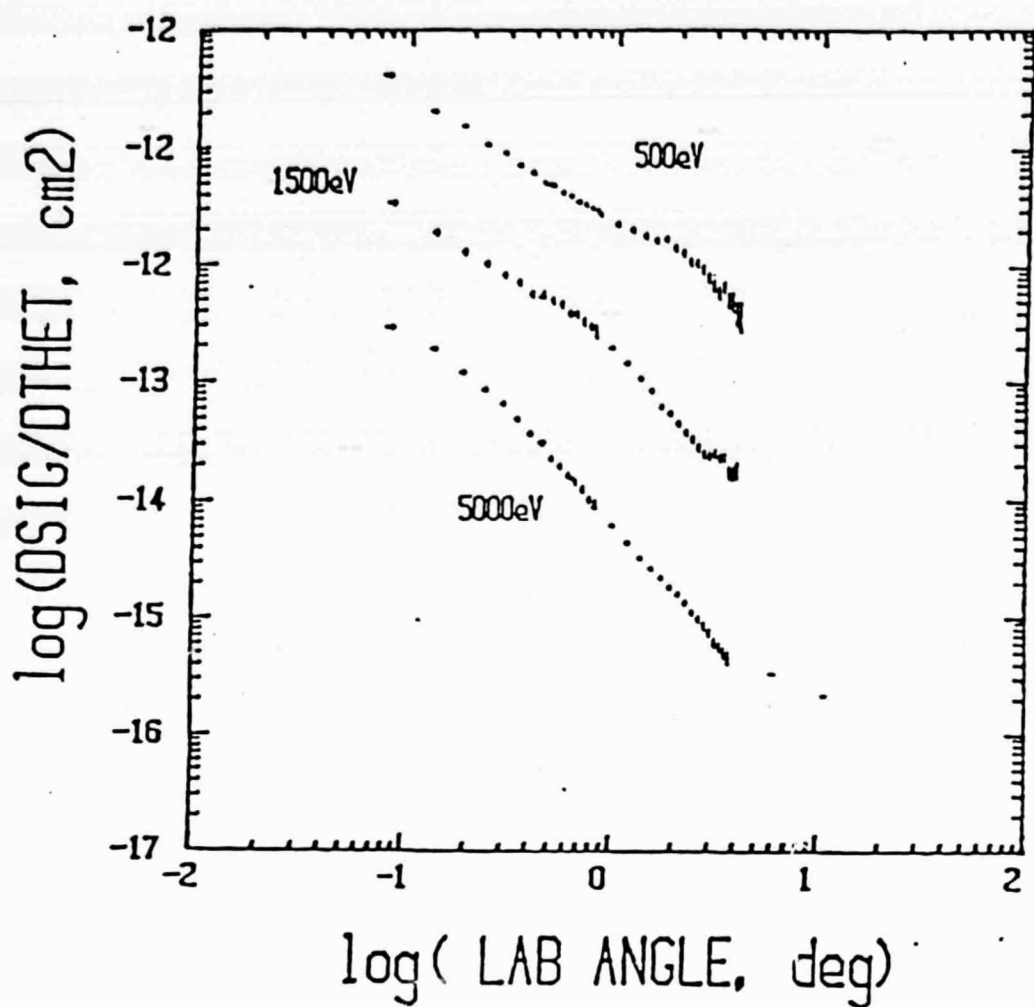


Fig. 12. Differential cross sections for angular scattering of ground-state 0.5-, 1.5-, and 5-keV oxygen atoms by O₂.

O + He

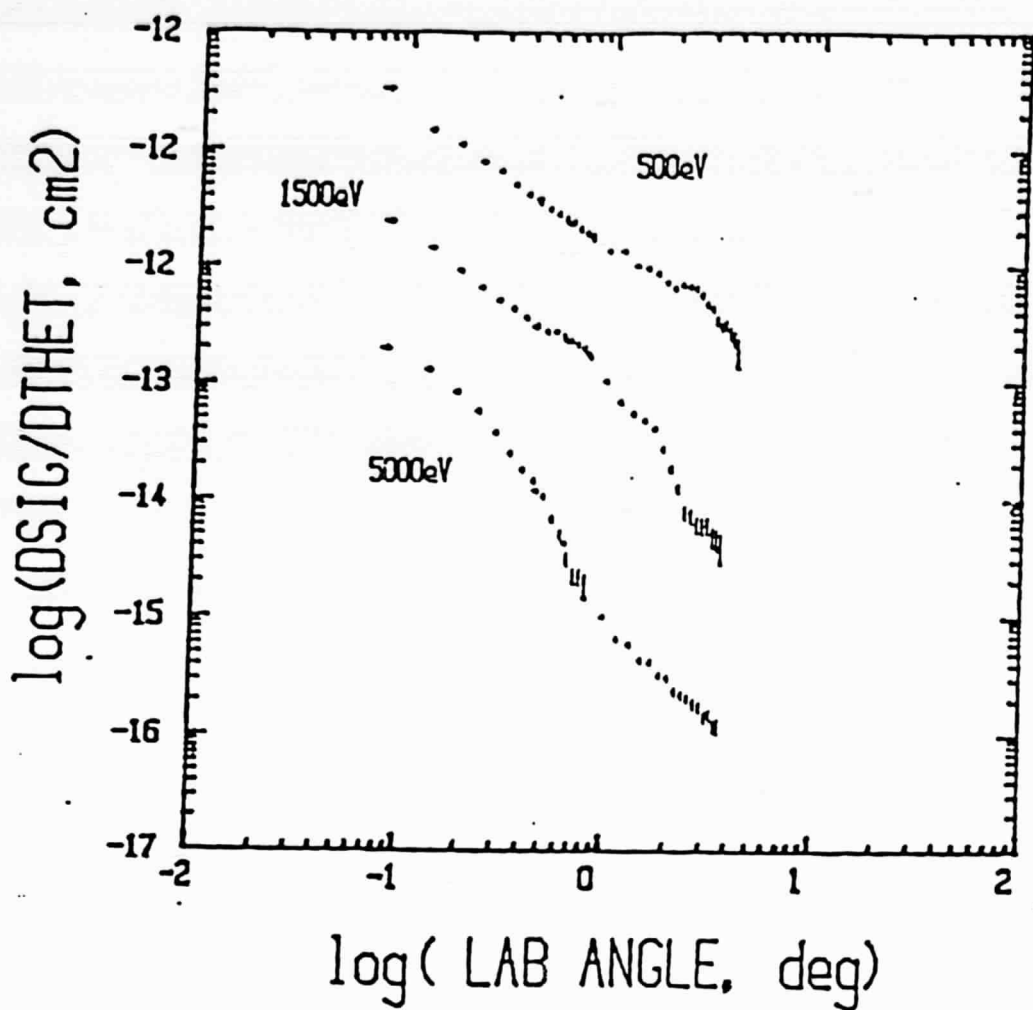


Fig. 13. Differential cross sections for angular scattering of ground-state 0.5-, 1.5-, and 5-keV oxygen atoms by He

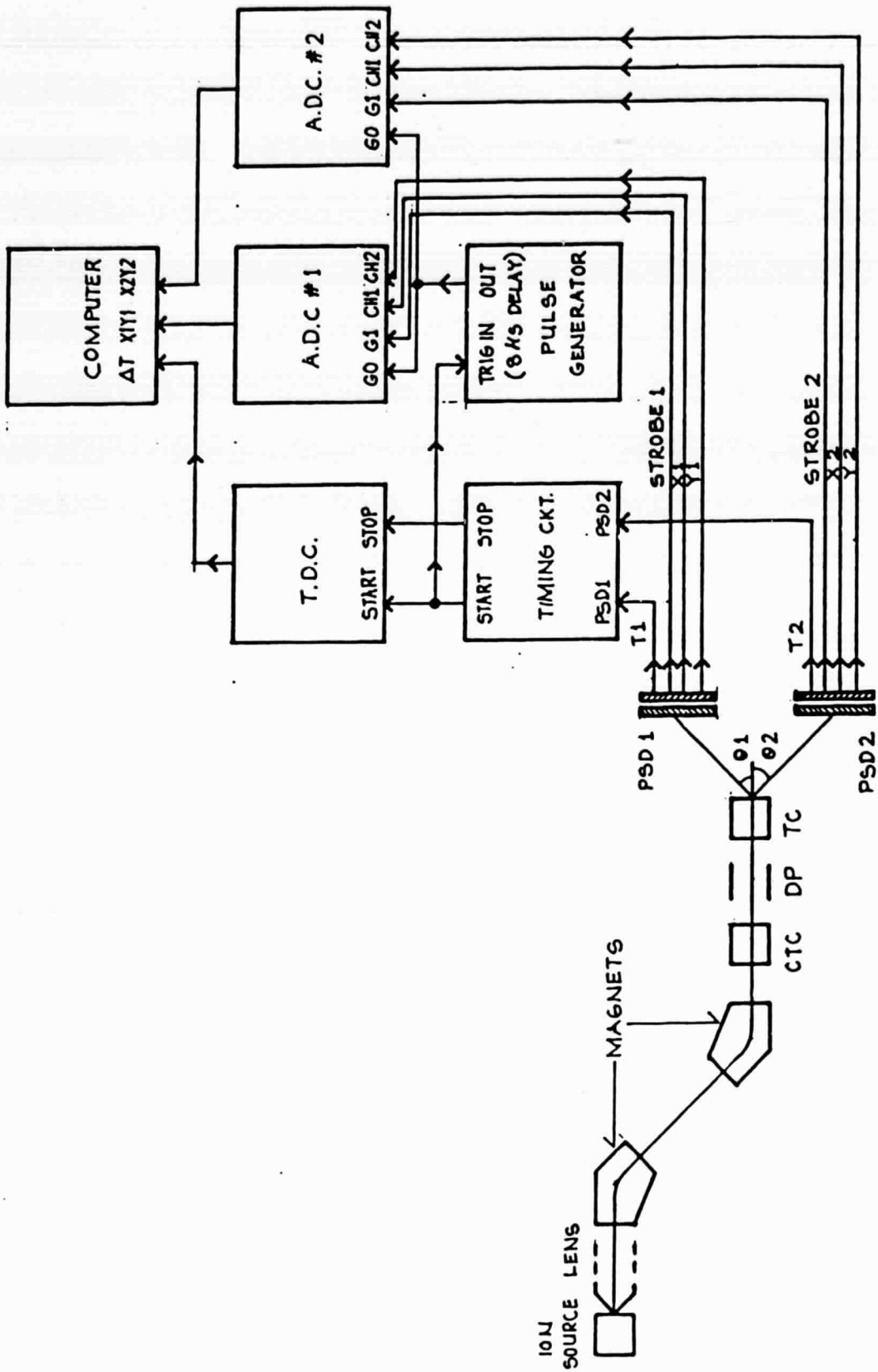


Fig. 14. Apparatus for study of large-angle scattering. Both particles from a single collision event are detected in coincidence.

He4 (3000eV) + He4

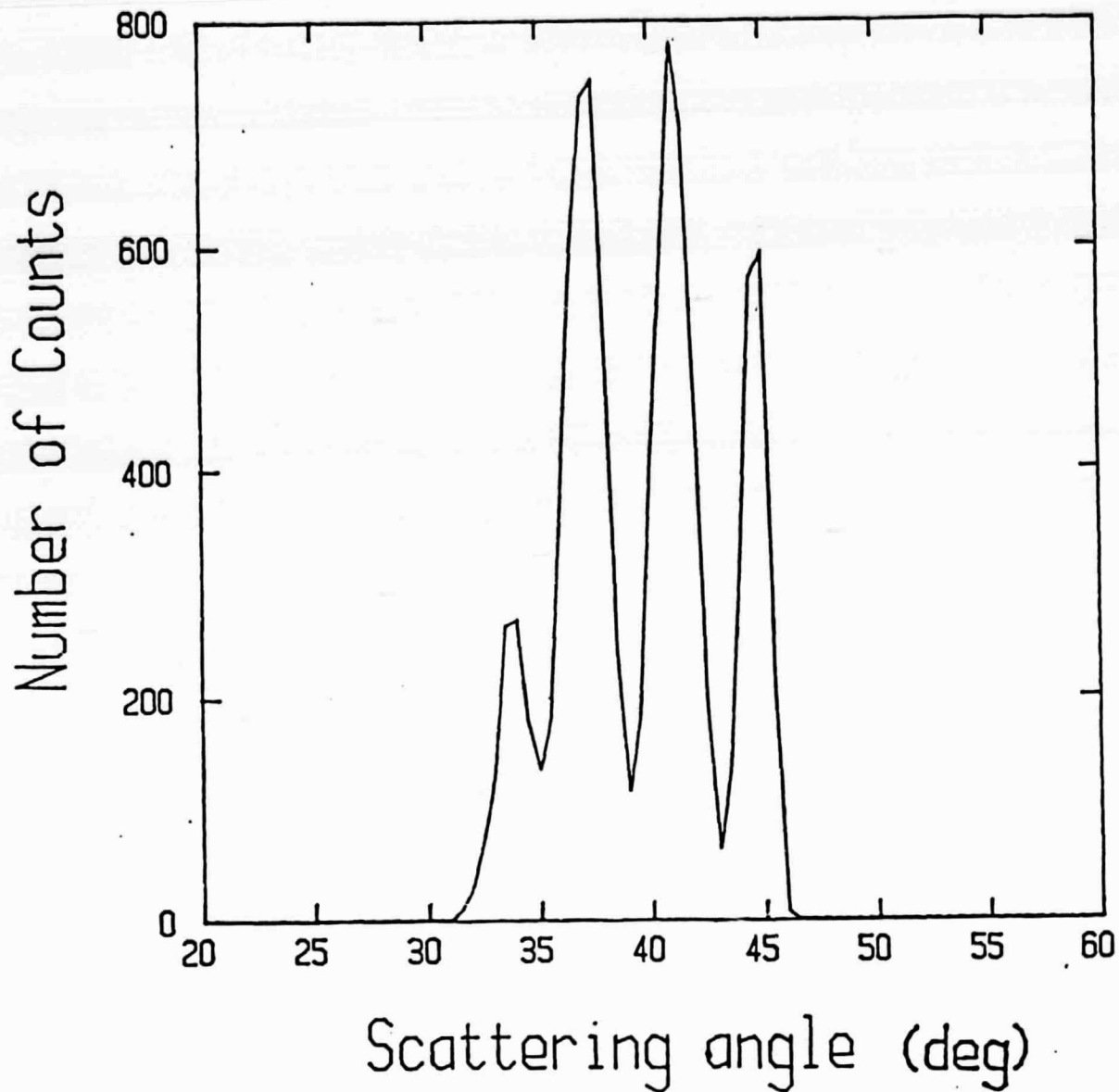


Fig. 15. Relative differential cross section for large-angle scattering of 3-keV ${}^4\text{He}$ from a thermal ${}^4\text{He}$ target. The large oscillations in the cross section arise because the colliding nuclei are indistinguishable.

He3 (3000eV) + He4

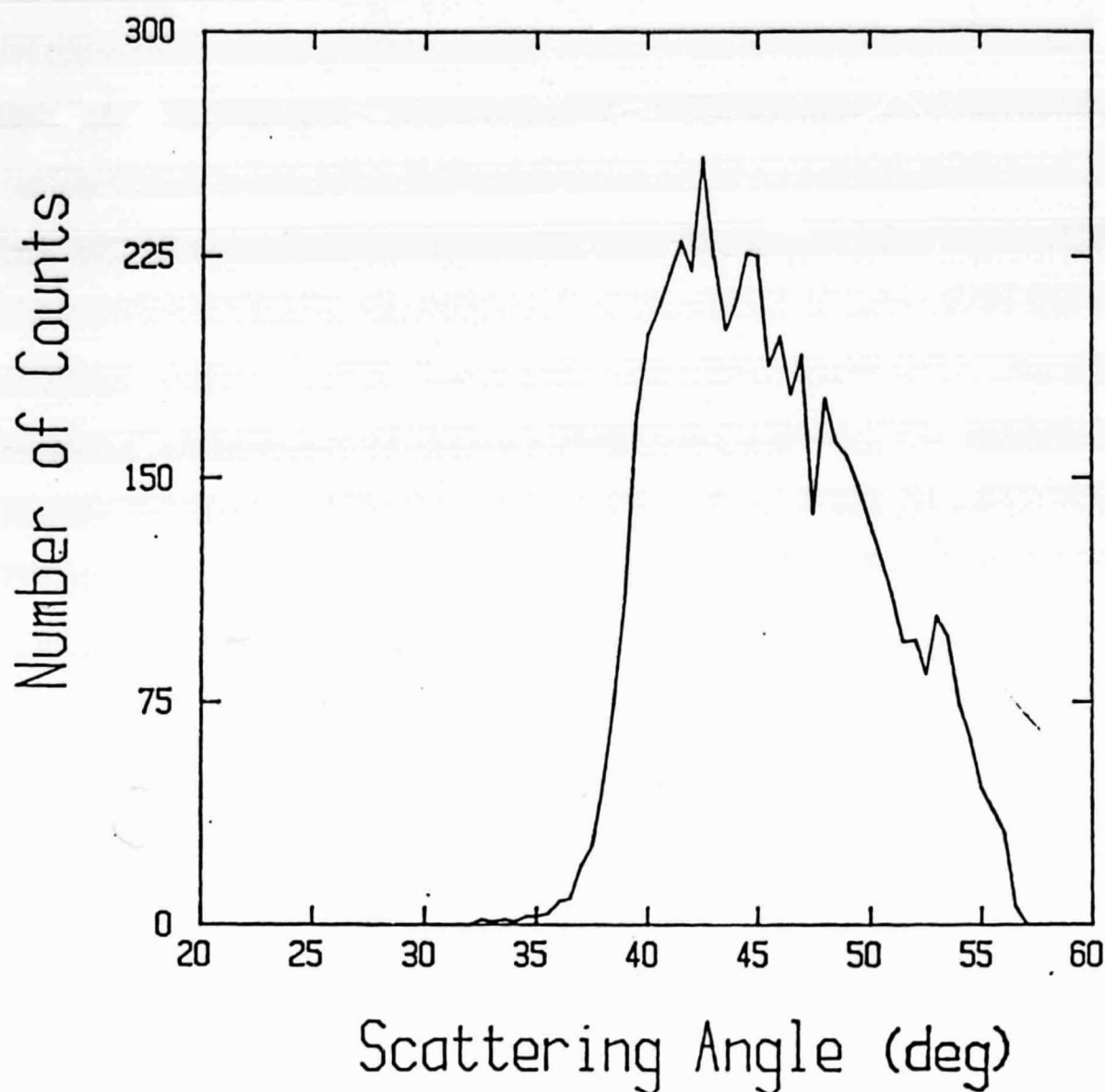


Fig 16. Relative differential cross section for large-angle scattering of 3-keV ^3He from a thermal ^4He target. The oscillations are absent because the nuclei are distinguishable.